Supporting Information

Amorphous vanadium-doped iron borate/tetra boride hybrid as efficient electrocatalyst for oxygen evolution reaction

Tanbir Ahmed, [a,b] Santanu Pal, [a,b] Nibedita Sinha, [a,b] Chandni Das [a, b] and Poulomi Roy *[a,b]

[a] Physical and Materials Chemistry Division, CSIR- National Chemical Laboratory (NCL), Pune 411008 Maharashtra, India.

[b]Academy of Scientific and Innovative Research (AcSIR), Ghaziabad, Uttar Pradesh 201002, India.

*Email: poulomiroy@yahoo.com, r.poulomi@ncl.res.in

Figures

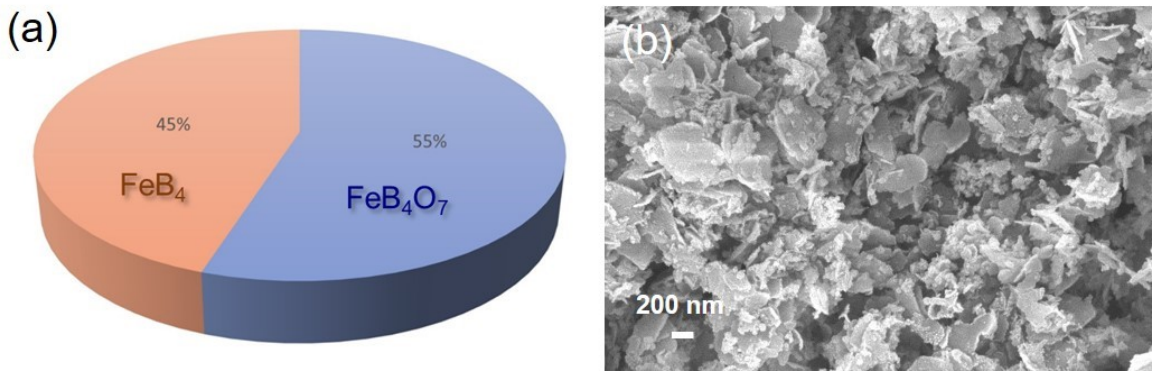

Fig. S1 (a) Pie chart representing phase quantification of FB sample and (b) corresponding FESEM image.

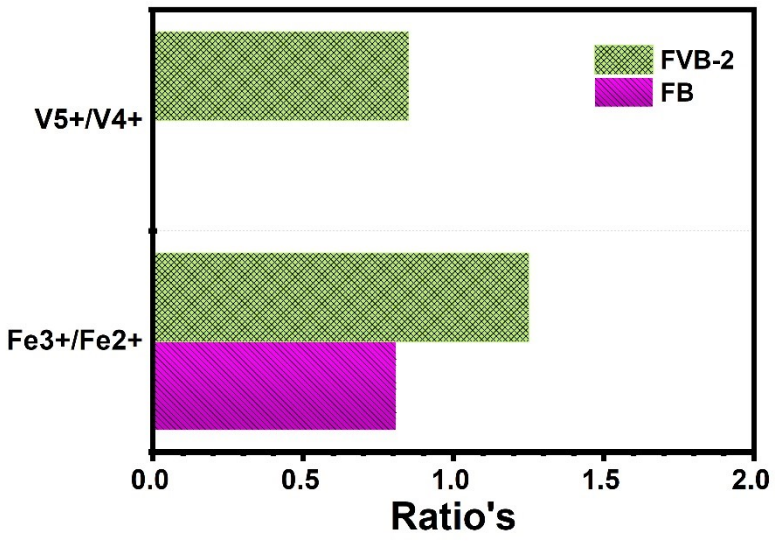

Fig. S2 Bar graph representation of ratios of metal species in their various oxidation states between FB and FVB-2.

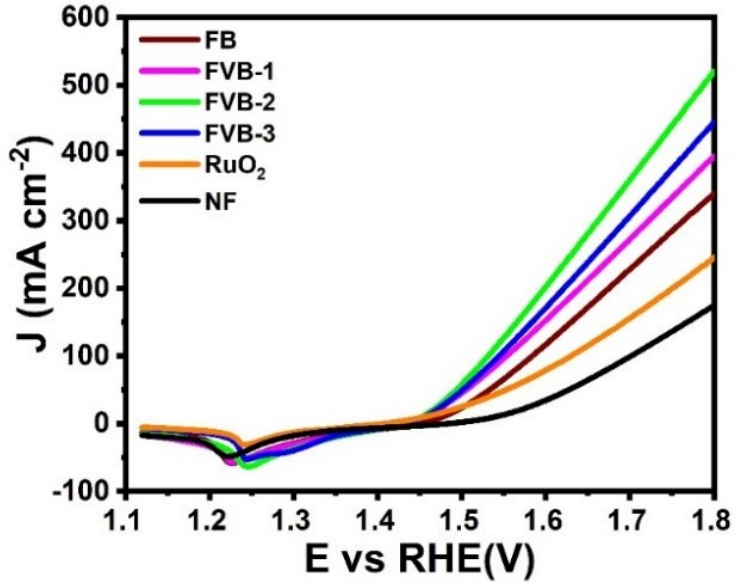

Fig. S3 LSV plots of developed electrocatalysts as well as conventional RuO_2 and bare Ni foam without iR correction in 1M KOH electrolyte.

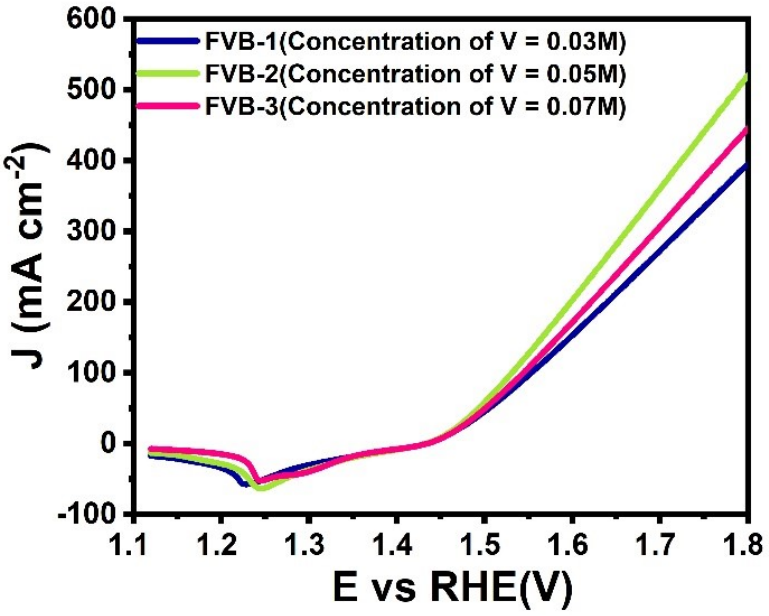

Fig. S4 LSV plots of developed electrocatalysts with three different doping concentration of vanadium.

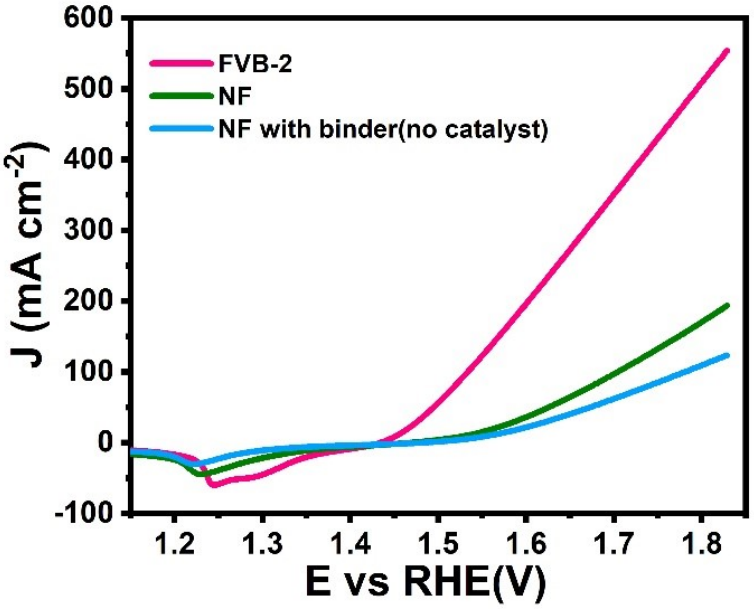

Fig. S5 LSV polarization curve of FVB-2, bare Ni foam (NF) and NF with identical mass loading of binder only (no catalyst) in 1 M KOH electrolyte medium.

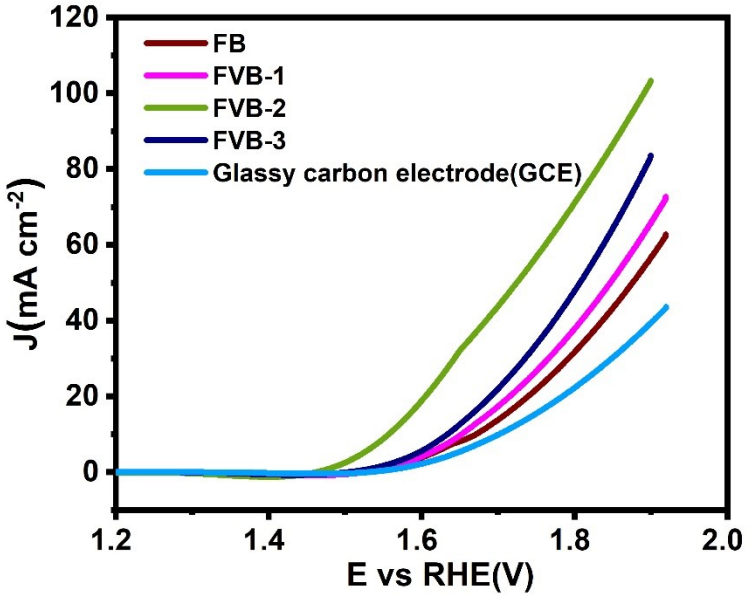

Fig. S6 LSV polarization curve of FB, FVB-1, FVB-2 and FVB-3 loaded on glassy carbon electrode in 1 M KOH electrolyte.

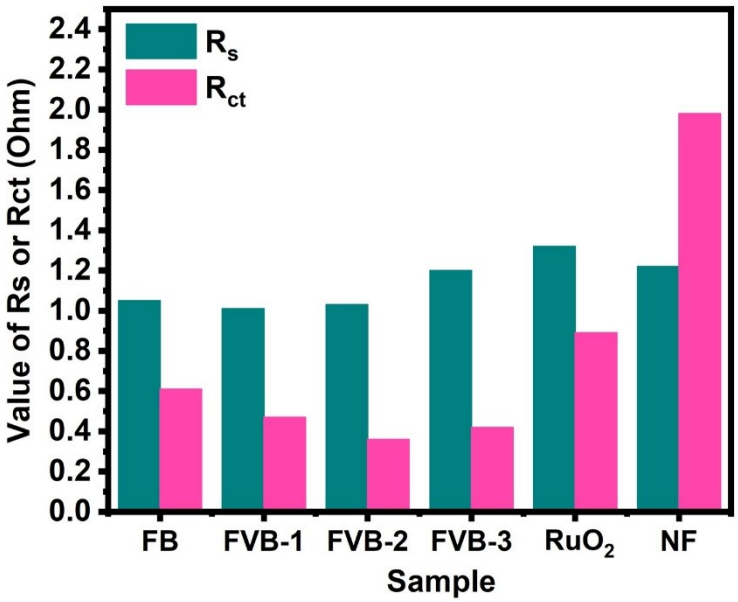

Fig. S7 Comparison of R_s and R_{ct} values of developed electrocatalyst derived from Nyquist plots.

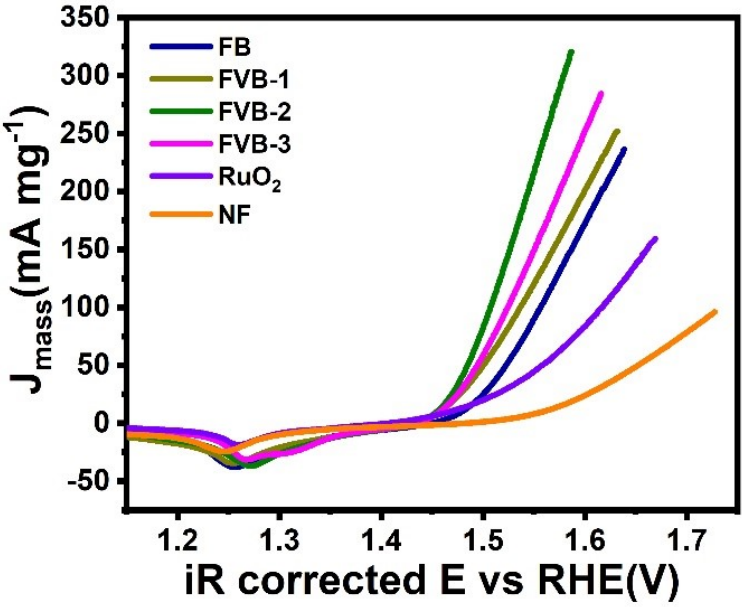

Fig. S8 Mass activity normalized LSV plot of developed electrocatalysts.

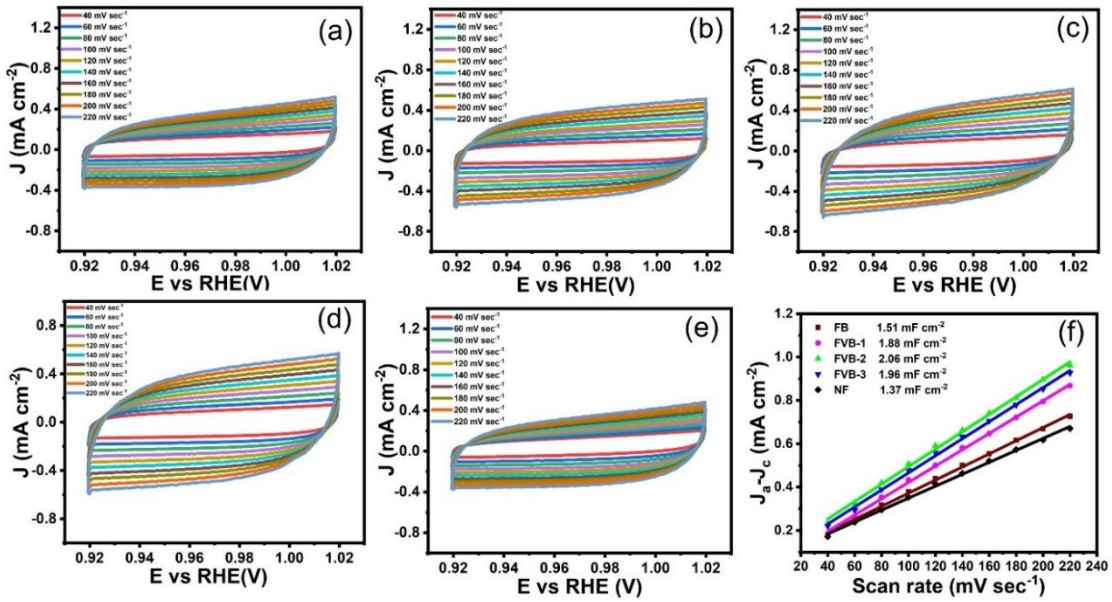

Fig. S9 Cyclic voltammograms (CV) obtained for (a) FB, (b) FVB-1, (c) FVB-2, (d) FVB-3 and (e) Nickel foam (NF) electrodes at different scan rates of 40-220 mV sec^{-1} in non-faradaic region for OER process in 1 M KOH electrolyte. (f) Plot of current density differences between anodic and cathodic peaks to determine the double layer (C_{dl}) capacitance values of different electrocatalysts toward OER in 1 M KOH.

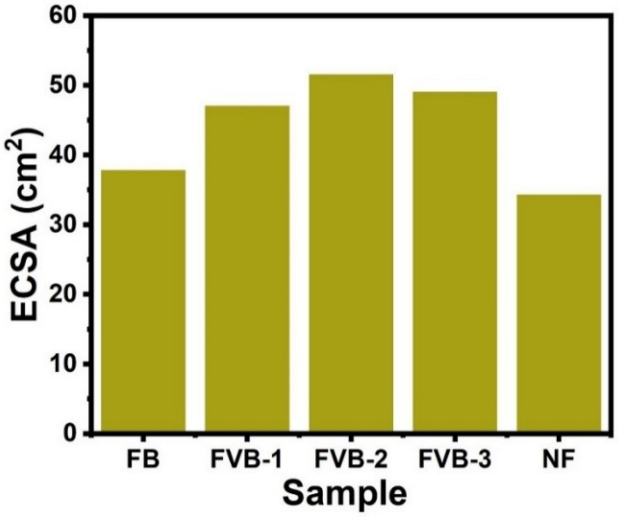

Fig. S10 Electrochemical active surface area (ECSA) plots of all developed electrocatalysts and bare Ni foam (NF) in 1 M KOH electrolyte solution for OER process.

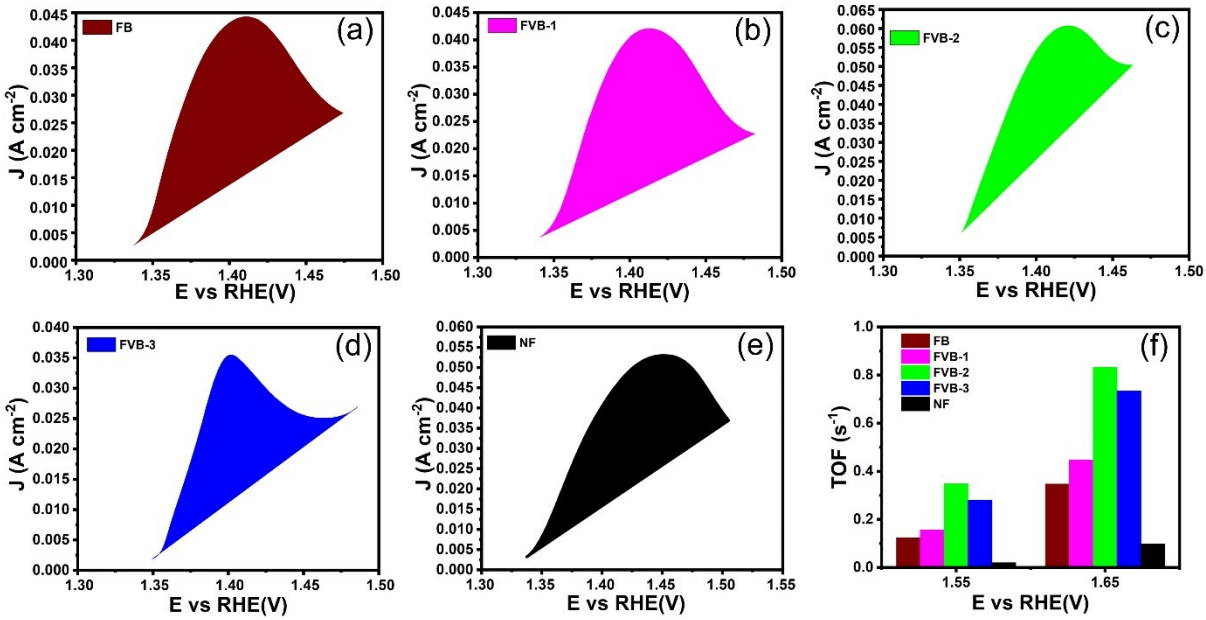

Fig. S11 Oxidation peak area of the CV curves taken at 20 mV s^{-1} scan rates for (a) FB, (b) FVB-1, (c) FVB-2 and (d) FVB-3 and (e) Nickel Foam (NF) in 1 M KOH electrolyte. (f) Calculated TOF values of prepared electrocatalysts for OER at different potentials.

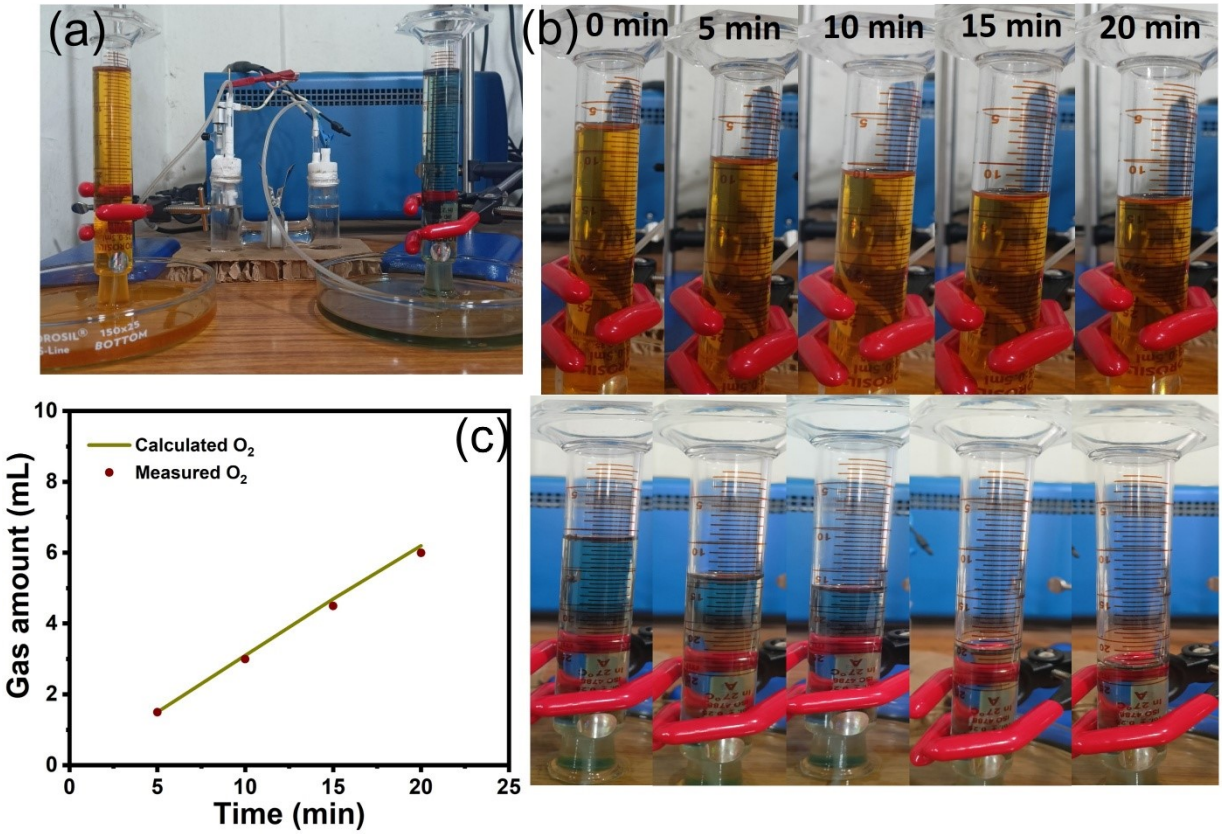

Fig. S12 (a) Optical image of the H-cell configuration employed for Faradaic efficiency measurements in alkaline electrolyte, showing the quantified collection of O_2 (yellow) and H_2 gases (no color) at regular 5-min intervals by volume replacement method (b). (c) Faradaic efficiency evaluated for OER mechanism under constant current density of 100 mA cm^{-2} in alkaline medium.

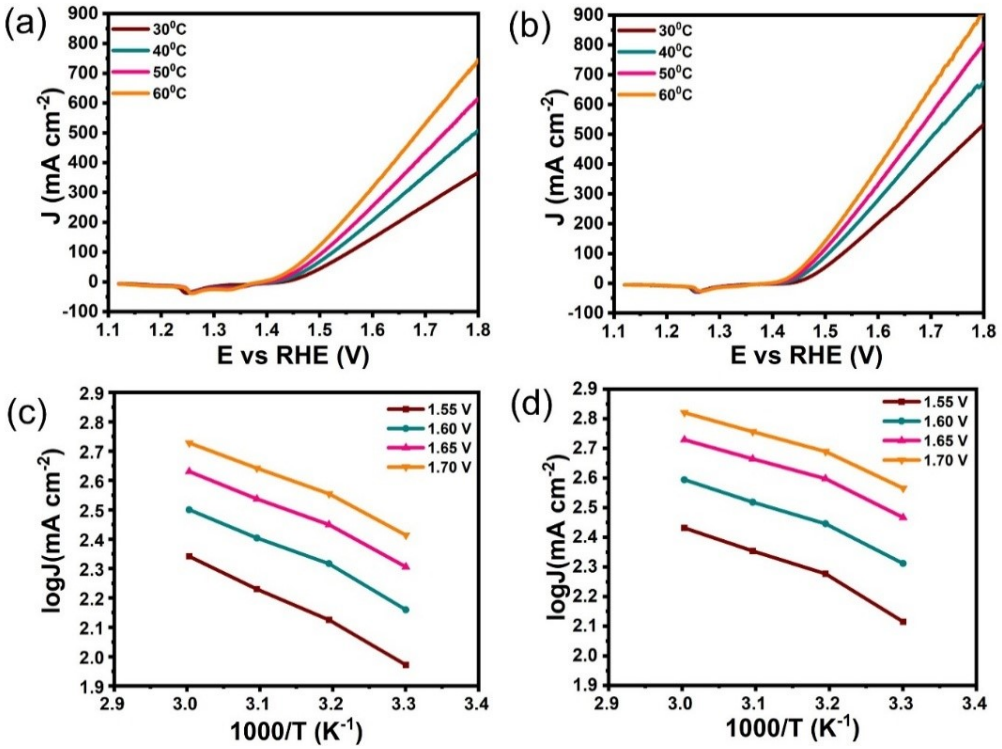

Fig. S13 (a, b) LSV plots for OER at different operational temperatures for FB (a) and FVB-2 (b). (c, d) Arrhenius plots at different oxidation potentials to determine activation energies for FB (c) and FVB-2 (d).

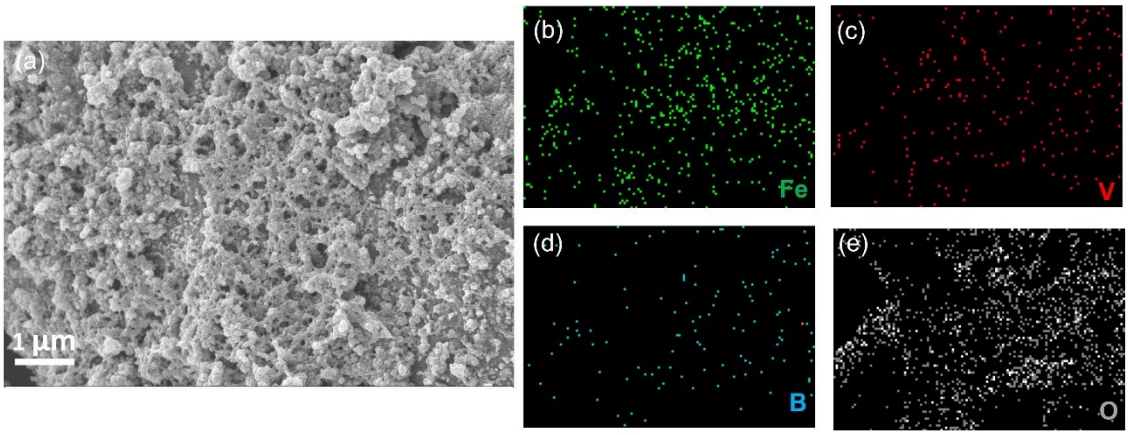

Fig. S14 (a) FESEM image and (b-e) Corresponding elemental mapping of FVB-2 after 48 h stability test in 1 M KOH electrolyte.

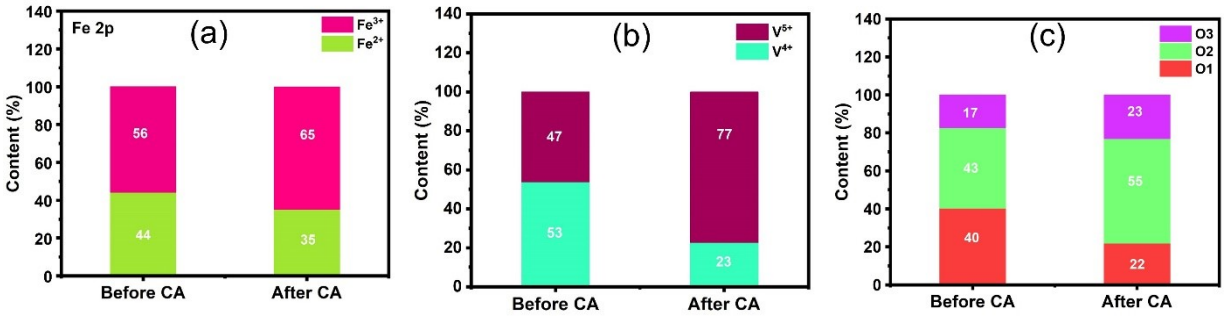

Fig. S15 Percentage of elements in different oxidation states obtained from XPS analysis for FVB-2 before and after stability test.

Tables

Table S1. Reaction parameters for the synthesis of various material.

Sample code	Reaction condition	Fe precursor	V precursor	$NaBH_4$
FB	In ice bath	0.10 M	-	0.5 M
FVB-1		0.07 M	0.03 M	
FVB-2		0.05 M	0.05 M	
FVB-3		0.03 M	0.07 M	

Table S2. Atomic % of FVB-2 from XPS Analysis

Sample	Atomic % Of elements			
	Fe 2p	V 2p	O 1s	B 1s
FVB-2	6.67	1.43	72.11	19.78

Table S3. The details of deconvoluted O 1*s* spectra for FB and FVB-2 sample.

Deconvoluted peaks	Sample	Peak area of O1	Peak area of O2	Peak area of O3	Total area	Ratio for O1	Ratio for O2	Ratio for O3
O 1s spectra	FB	55561	118067	103043	276671	0.2008	0.4267	0.3724
	FVB-2	107682	79838	30176	217696	0.4946	0.3667	0.1386

Table S4. R_s and R_{ct} values for developed electrocatalysts derived from Nyquist plots.

Materials	In 1M KOH	
	R_S (Ohm)	**R_{ct} (Ohm)**
FB	1.05	0.61
FVB-1	1.01	0.47
FVB-2	1.03	0.36
FVB-3	1.20	0.42
RuO_2	1.32	0.89
NF	1.22	1.98

Table S5. Comparative table for electrocatalytic OER activity of developed electrodes in 1 M KOH electrolyte medium in a three-electrode system.

Sample	η@10 mA cm^{-2} (mV)	η@100 mA cm^{-2} (mV)	Tafel slope (mV dec^{-1})	C_{dl} (mF cm^{-2})	ECSA (cm^2)	TOF (S^{-1}) @ 1.65V vs. RHE
FB	251	303	75.7	1.51	37.75	0.3474
FVB-1	233	279	67.3	1.88	47	0.4466
FVB-2	215	256	43.9	2.06	51.5	0.832
FVB-3	231	271	64.0	1.96	49	0.7338
NF	315	408	103.1	1.37	34.25	0.0975

Table S6. Comparative Table of oxidation potential of FVB-2 achieved at different current densities using 1 M KOH electrolyte medium in three electrode system.

Current density ($mA\ cm^{-2}$)	**iR compensated oxidation potential (V) In 1M KOH**
10	1.445
20	1.453
50	1.468
100	1.486
150	1.498
200	1.509
250	1.519

Table S7. Comparative OER performance of reported boride or borate based electrocatalysts in 1M KOH electrolyte.

Materials	Electrolyte	Overpotential η@ mA cm^{-2}	Tafel slope (mV dec^{-1})	Stability	Ref.
FVB-2	**1 M KOH**	**215@10 mA cm^{-2}**	**43.9**	**48 h @ 200 mA cm^{-2}**	**This work**
FeB_2 NPs	1 M KOH	296@10 mA cm^{-2}	52.4	1000 cycles	1
VCNB	1 M KOH	340@10 mA cm^{-2}	58	10 h@100 mA cm^{-2}	2
Co2-Fe-B	1 M KOH	298@10 mA cm^{-2}	62.6	12 h@10 mA cm^{-2}	3
Co-Fe-Bi/NF	1 M KOH	307@10 mA cm^{-2}	68.6	40 h@10 mA cm^{-2}	4
Co-Mo-B NPs	1 M KOH	320@10 mA cm^{-2}	155	10 h@20 mA cm^{-2}	5
Nickel borate on Ni_3B	1 M KOH	302@10 mA cm^{-2}	52	8 h@10 mA cm^{-2}	6
Co-B@Co-B_i	1 M KOH	291@10 mA cm^{-2}	105	5000 cycles	7
$FeNi_3$-B/G nanosheets	1 M KOH	230@15 mA cm^{-2}	50	12 h@10 mA cm^{-2}	8
NiFeB@$NiFeB_i$	1 M KOH	237@10 mA cm^{-2}	57.65	2000 cycles	9
Ni_3B/rGO	1 M KOH	290@10 mA cm^{-2}	88.4	12 h@10 mA cm^{-2}	10
Co-Bi NS/G nanosheet	1 M KOH	290@10 mA cm^{-2}	53	1000 cycles	11
Fe–B–O@Fe_2B	1 M KOH	260@10 mA cm^{-2}	57.9	500 cycles	12
Co-Ni-B	1 M KOH	313@10 mA cm^{-2}	120	12 h@10 mA cm^{-2}	13
WFeNiB/NF	1 M KOH	223@10 mA cm^{-2}	38.8	12 h@100 mA cm^{-2}	14
NiCoFeB	1 M KOH	284@10 mA cm^{-2}	46	20 h @10 mA cm^{-2}	15

References:

1. H. Li, P. Wen, Q. Li, C. Dun, J. Xing, C. Lu, S. Adhikari, L. Jiang, D.L. Carroll and S.M. Geyer, *Adv. Energy Mater.,* 2017, **7**, 1700513.
2. H. Han, Y.R. Hong, J. Woo, S. Mhin, K. M. Kim, J. Kwon, H. Choi, Y.C. Chung and T. Song, *Adv. Energy Mater.,*2019,**9**,1803799.
3. H. Chen, S. Ouyang, M. Zhao, Y. Li and J. Ye, *ACS Appl. Mater. Interfaces.,* 2017, **9**, 40333-40343.
4. U. P. Suryawanshi, M. P. Suryawanshi, U. V. Ghorpade, S. W. Shin, J. Kim and J. H. Kim, *Appl. Surf. Sci.,* 2019,**495**, 143462.
5. S. Gupta, N. Patel, R. Fernandes, S. Hanchate, A. Miotello and D.C. Kothari, *Electrochim. Acta.,* 2017, **232**, 64-71.
6. W.J. Jiang, S. Niu, T. Tang, Q.H. Zhang, X.Z. Liu, Y. Zhang,Y.Y. Chen, J.H. Li, L.Gu, L.J. Wan and J.S. Hu, *Angew. Chem. Int. Ed.,* 2017, **56**, 6572-6577.
7. T. Tan, P. Han, H. Cong, G. Cheng and W. Luo, *ACS Sustain. Chem. Eng.*, 2019, **7**, 5620-5625.
8. J.M.V. Nsanzimana, R. Dangol, V. Reddu, S. Duo, Y. Peng, K.N. Dinh, Z. Huang, Q. Yan and X. Wang, *ACS Appl. Mater. Interfaces.,* 2018, **11**, 846-855.
9. P.Han, T.Tan, F.Wu, P.Cai, G.Cheng and W. Luo,*Chin. Chem. Lett.,* 2020, **31**, 2469-2472.
10. M. Arivu, J. Masud, S. Umapathi and M. Nath, Electrochem. commun., 2018, **86**, 121-125.
11. P.Chen, K. Xu, T. Zhou, Y. Tong, J. Wu, H. Cheng, X. Lu, H. Ding, C. Wu and Y. Xie, *Angew. Chem. Int. Ed.,* 2016, **55**, 2488-2492.
12. L. Wang, J. Li, X. Zhao, W. Hao, X. Ma, S. Li and Y. Guo, *Adv. Mater. Interfaces.,* 2019, **6**, 1801690.
13. N. Xu, G. Cao, Z. Chen, Q. Kang, H. Dai and P. Wang, *J. Mater. Chem. A*, 2017,**5**, 12379-12384.
14. Y. Sun, Y. Zhao, X. Deng, D. Dai and H. Gao, *Sustain. Energy Fuels,* 2022, **6**, 1345-1352.
15. Y. Li, B. Huang, Y. Sun, M. Luo, Y. Yang, Y. Qin, L. Wang, C. Li, F. Lv, W. Zhang and S. Guo, *Small,* 2019, **15**, 1804212.